# Activation of Highly Ordered Pyrolytic Graphite for Heterogeneous Electron Transfer: Relationship between Electrochemical Performance and Carbon Microstructure

**Robert J. Bowling, Richard T. Packard, and Richard L. McCreery***

*Contribution from the Department of Chemistry, The Ohio State University, 120 West 18th Avenue, Columbus, Ohio 43210.* *Received May 26, 1988. Revised Manuscript Received September 8, 1988*

**Abstract:** The electrochemical and vibrational spectroscopic properties of highly ordered pyrolytic graphite (HOPG) were determined before and after modification by anodization or pulsed laser irradiation. Both treatments greatly accelerated the heterogeneous electron transfer rate constants for the $Fe(CN)_6^{3-/4-}$ and dopamine redox systems on HOPG by approximately six orders of magnitude. Modification also caused significant changes in the Raman spectrum of HOPG, with new bands appearing at 1360 and 1605 $cm^{-1}$ for both pretreatments. The 1360-$cm^{-1}$ band is spectroscopically indicative of graphitic edge plane, and the results indicate that electron transfer activation correlates with edge plane density. The intensity of the 1360-$cm^{-1}$ band correlated with electron transfer activation, with a high intensity corresponding to higher $k^0$ for either electrochemical or laser pretreatment. At intermediate electrochemical pretreatment (ECP) potentials, a spatially heterogeneous surface resulted, with surface regions exhibiting the 1360-$cm^{-1}$ band being separated by tens of microns. Such heterogeneity was verified by voltammetry, with distinct waves being observed for active and inactive surface regions. Such heterogeneity was not observed for laser treated surfaces, with a sudden and spatially uniform activation occurring between 40 and 50 MW $cm^{-2}$. The results clearly indicate that graphitic edge plane is necessary for fast electron transfer, and that the pretreatment procedures accelerate $k^0$ by generating edge plane defects in the HOPG lattice. The mechanisms of defect generation for the two procedures appear very different, with ECP appearing to follow a nucleation process leading to a spatially heterogeneous surface, while the laser pulse appears to shatter the HOPG lattice, leading to a more uniform distribution of active sites. The results provide important conclusions about the relationship between carbon electrode microstructure and heterogeneous electron transfer activity.

A large body of literature has appeared over several decades on the electrochemical properties of carbon, with the most recent comprehensive review appearing in 1988.[1] The important commercial and analytical applications of carbon electrodes combined with complex and interesting surface chemistry have provided the driving force for examining the relationship between interfacial structure and electrochemical activity.[2-4] Of particular interest is the heterogeneous electron transfer rate between carbon electrodes and various well-known redox systems such as ascorbic acid, ferri/ferrocyanide, and the catecholamines. Not only are these systems of significant analytical interest, but they serve as benchmarks for comparisons of electrode performance. Until relatively recently, the observed heterogeneous rate constants for these redox systems ($k^0$'s) were extremely irreproducible (by factors of up to $10^3$) due to variations in surface history and carbon type. Such variation frustrated attempts to determine which aspects of surface structure or preparation determined the value of $k^0$, and any systematic examination of electrode kinetics on carbon was very difficult if not impossible.

With the development of heat treatment procedures,[5-9] ultraclean polishing techniques,[10,11] and electrochemical activation,[12-20] it became possible to prepare reproducibly active carbon surfaces, particularly from glassy carbon substrates. With adequate care, glassy carbon exhibits a $k^0$ value for the ferri/ferrocyanide redox system close to that for platinum, and 10–1000 times faster than less successful pretreatment procedures.[7,8] Our group added to the list of successful pretreatments by reporting that intense laser pulses can activate glassy carbon at least as well as other methods, with activation occurring in situ, repeatedly if desired.[21-24] While careful polishing, heat treatment, electrochemical anodization, and laser activation result in roughly comparable increases in $k^0$ for several benchmark systems, there are major differences in surface chemistry for the various methods. Vacuum heat treatment and laser activation have low apparent capacitance (ca. 20 $\mu F/cm^2$)[6,24] while polishing and electrochemical pretreatment lead to much higher values (70–200 $\mu F/cm^2$).[8,24] Polished surfaces exhibit a pH dependent $k^0$ for ferri/ferrocyanide,[25] while laser treated surfaces do not.[24] Polished or electrochemically pretreated surfaces exhibit a pH dependent quinone-like surface bound redox couple, while heat or laser treated GC do not.[6,8,12,20,24] Electro-

* Author to whom correspondence should be addressed.

(1) Kinoshita, K. *Carbon: Electrochemical and Physicochemical Properties*; Wiley: New York, 1988.
(2) Sarangapani, S.; Akridge, J. R.; Schumm, B., Eds. *Proceedings of the Workshop on the Electrochemistry of Carbon*; The Electrochemical Society: Pennington, NJ, 1984.
(3) Randin, J.-P. In *Encyclopedia of Electrochemistry of the Elements*; Bard, A. J., Ed.; Dekker: New York, 1976; Vol. 7, pp 1–291.
(4) Besenhard, J. O.; Fritz, H. P. *Agnew. Chem., Int. Ed. Engl.* **1983**, *22*, 950.
(5) Stutts, K. J.; Kovach, P. M.; Kuhr, W. G.; Wightman, R. M. *Anal. Chem.* **1983**, *55*, 1632.
(6) Fagan, D. T.; Hu, I. F.; Kuwana, T. *Anal. Chem.* **1985**, *57*, 2759.
(7) Wightman, R. M.; Deakin, M. R.; Kovach, P. M.; Kuhr, W. G.; Stutts, K. J. *J. Electrochem. Soc.* **1984**, *131*, 1578.
(8) Hu, I-F.; Kuwana, T. *Anal. Chem.* **1986**, *58*, 3235.
(9) Deakin, M. R.; Kovach, P. M.; Stutts, K. J.; Wightman, R. M. *Anal. Chem.* **1986**, *58*, 1474.
(10) Hu, I. F.; Karweik, D. H.; Kuwana, T. *J. Electroanal. Chem.* **1985**, *188*, 59.
(11) Kazee, B.; Weisshaar, D. E.; Kuwana, T. *Anal. Chem.* **1985**, *57*, 2739.
(12) Engstrom, R. C.; Strasser, V. A. *Anal. Chem.* **1984**, *56*, 136.
(13) Engstrom, R. C. *Anal. Chem.* **1982**, *54*, 2310.
(14) Kovach, P. M.; Deakin, M. R.; Wightman, R. M. *J. Phys. Chem.* **1986**, *90*, 4612.
(15) Wang, J.; Hutchins, L. O. *Anal. Chim. Acta* **1985**, *167*, 325.
(16) Cabaniss, G. E.; Diamantis, A. A.; Murphy, W. R., Jr.; Linton, R. W.; Meyer, T. J. *J. Am. Chem. Soc.* **1985**, *107*, 1845.
(17) Falat, L.; Cheng, H. Y. *J. Electroanal. Chem.* **1983**, *157*, 393.
(18) Gonon, F. G.; Fombarlet, C. M.; Buda, M. J.; Pujol, J. F. *Anal. Chem.* **1981**, *53*, 1386.
(19) Wightman, R. A.; Paik, E. C.; Borman, S.; Dayton, M. A. *Anal. Chem.* **1978**, *50*, 1410.
(20) Kepley, L. J.; Bard, A. J. *Anal. Chem.* **1988**, *60*, 1459.
(21) Hershenhart, E.; McCreery, R. L.; Knight, R. D. *Anal. Chem.* **1984**, *56*, 2256.
(22) Poon, M.; McCreery, R. L. *Anal. Chem.* **1986**, *58*, 2745.
(23) Poon, M.; McCreery, R. L. *Anal. Chem.* **1987**, *59*, 1615.
(24) Poon, M. J.; McCreery, R. L.; Engstrom, R. *Anal. Chem.* **1988**, *60*, 1725.
(25) Deakin, M. R.; Stutts, K. J.; Wightman, R. M. *J. Electroanal. Chem.* **1985**, *182*, 113.

0002-7863/89/1511-1217$01.50/0 

chemical pretreatment of GC produces a porous, hydrated film up to at least 0.9 μm in thickness,[20] yet there is no evidence for such a film on laser treated or VHT surfaces. Severe electrochemical pretreatment leads to a partially insulating surface which retains high $k^0$ over a fraction of its surface.[14] These observations indicate that different procedures yield structurally distinct surfaces, and the question of which surface structural properties are necessary for rapid $k^0$ remains unanswered.

Both the recent and older literature discuss the possibility that active sites may exist on carbon, and activation procedures may produce or uncover such sites. Kuwana et al. concluded that heat treatment removed oxygen functional groups and impurities from GC, and that activation resulted from a clean surface containing active sites.[6,8,10] Wightman came to a similar conclusion,[14] while other workers have attributed activation to oxygen functional groups[16,26-29] or exposure of the underlying GC substrate structure.[30] It has long been observed that exposed graphitic edges correlate with electron transfer activation. For example, the ferri/ferrocyanide redox system exhibits a 3-fold higher exchange current on edge vs basal plane graphite,[31] and exposure of edge plane has been proposed as the mechanism of several activation procedures.[1,3,7] In none of the previous reports on carbon activation has there been a direct correlation between the population of active sites and electron transfer activation. The objective of the present work was the investigation of the relationship between a spectroscopically observable surface feature and the observed $k^0$ value. In particular, we sought to explain the origin of $k^0$ enhancement by laser activation.

The approach presented here differs from the large bulk of previous investigations in three ways. First, the electrode material was highly ordered pyrolytic graphite (HOPG) rather than glassy carbon. Unlike GC, HOPG is a microstructurally well-defined material, and the initial surface structure is known, at least before activation. Second, we used Raman spectroscopy as a probe of carbon microstructure, to permit structural inferences during and after activation. Third, we used both laser activation and electrochemical pretreatment (ECP) to modify the HOPG surface. Both methods provide a controlled, and in certain cases gradual, means to alter the HOPG surface, permitting correlations between spectral changes and $k^0$ enhancement.

## Experimental Section

HOPG was a gift from Arthur Moore at Union Carbide, Parma, Ohio, and the GC was Tokai GC 20S. A fresh HOPG surface was exposed by removal of superficial layers with common adhesive tape, and the GC20S was polished conventionally with the final abrasive being 0.05-μm alumina. Electrochemical apparatus was conventional, consisting of a Princeton Applied Research Corporation 173/176 potentiostat controlled by a PC compatible computer and Tecmar Labmaster analog interface. HOPG was mounted in a Kel-F holder and the active electrode region was defined by a viton o-ring which prevented solution contact with the edge plane. The exposed basal plane area was 0.70 $cm^2$ for ECP experiments. ECP was conducted with a procedure similar to that of Engstrom,[12,13] with a 2 min controlled potential anodization in 0.1 M $KNO_3$ followed by a cathodic step to −0.1 V vs Ag/AgCl for 30 s. For voltammetry, a small o-ring defined a $7.8 \times 10^{-3}$ $cm^2$ electrode area, and potentials are referred to the Ag/AgCl (3 M NaCl) electrode. Laser pretreatment was conducted with three pulses (1064 nm, 9 ns) on a bare, freshly peeled HOPG surface in air. Raman spectra were obtained with a $Ar^+$ laser beam reflected from the center of the laser activated spot. For voltammetry, an o-ring was placed at the center of the laser spot, defining a $7.8 \times 10^{-3}$ $cm^2$ electrode area. Reported power densities are accurate to ±20% and were measured at the center 1 mm of the laser beam to maximize beam uniformity.[23,24] Raman spectra were obtained with an unmodified Spex 1403 spectrometer with a Spex 1482A microprobe and 31034A single photon detector, or with a custom high sensitivity multichannel spectrometer described previously (ref[32], spectrometer "C"). ECP or laser activated carbon surfaces were sensitive to laser damage during spectroscopy, so low laser power (ca. 20 mW for gross sampling, 5 mW for microprobe) was important, as was multichannel detection. For both scanning and multichannel spectral acquisition, it was verified that the spectrum did not change with successive acquisitions. For all Raman spectra, the probe laser wavelength was 515 nm. The majority of the Raman spectra were obtained with a 100 μm × 1 mm laser spot size on the carbon sample, and these will be referred to as "gross" spectra. For "microprobe" spectra, the laser spot size was ca. 5 μm in diameter.

## Results

**Carbon Electrode Spectroscopy.** Raman spectra of carbon materials have been examined in some detail and are quite dependent on the origin of the material. Several spectra for the materials used here are shown in Figure 1. GC-20 shows a strong 1360-$cm^{-1}$ band,[33,36] and the 1580–1620-$cm^{-1}$ band is dependent on heat treatment temperature.[37] HOPG basal plane shows only a very weak 1360-$cm^{-1}$ band, plus the strong 1582-$cm^{-1}$ $E_{2g}$ mode.[38-41] Spectrum D of Figure 1 is a microprobe spectrum on a visible tear on the HOPG basal plane, shown in the SEM of Figure 2A. Such defects are infrequent, representing less than 1% of a carefully exposed surface. While the 1360-$cm^{-1}$ band for the defect is weak, its frequency matches that of the edge plane HOPG, shown in Figure 1C.[39] The 1360-$cm^{-1}$ mode has been assigned to the $A_{1g}$ mode expected for $D^4_{6h}$ symmetry and is Raman allowed only for small graphitic crystallites.[38] It is present wherever significant edge density is present, as in GC, edge plane HOPG, and the HOPG defect. The 1582-$cm^{-1}$ band is complex, being composed of two components.[36,42,43] For extremely disordered graphite[44] or intercalation compounds,[45] it shifts to higher wavenumber in a range of 1590–1630 $cm^{-1}$. This shift has been explained by attributing the higher energy band to "boundary layer" graphite, which is adjacent to zero or one neighboring graphitic planes. The ca. 1620-$cm^{-1}$ mode is prominent for graphitic planes bounded by intercalant layers and is the only band observed for Stage 1 intercalation compounds where the graphite layers are never adjacent to each other. The 1582-$cm^{-1}$ mode is attributed to "inner layer" graphite which is bounded by two adjacent graphite planes. In Stage 4 intercalation compounds, for example, the "inner layer" and "boundary layer" planes are equal in number and the 1582- and 1620-$cm^{-1}$ bands are equal in intensity.[45] The higher energy band frequency is dependent on sample history, and in the results reported here it occurred most frequently at 1605 $cm^{-1}$. For the purposes of this report, it is important to recognize the association of the 1360-$cm^{-1}$ band with the size of the graphitic plane, whereas the 1600–1630-$cm^{-1}$ mode is related to the stacking of graphite planes.

**Untreated HOPG Electrodes.** Basal plane HOPG exhibits poor electron transfer kinetics for dopamine and $Fe(CN)_6^{3-/4-}$, as shown in Figure 3a and reported by Wightman.[7,19] The anodic/cathodic peak separation for $Fe(CN)_6^{3-/4-}$ (1 M KCl) is >1.2 V at 0.1 V/s, corresponding to an approximate $k^0$ value of $<10^{-9}$ cm $s^{-1}$. The initial HOPG surface shows negligible edge plane Raman intensity at 1360 $cm^{-1}$, negligible 1620-$cm^{-1}$ intensity, and poor heterogeneous electron transfer kinetics.

**Laser-Treated HOPG.** When the HOPG surface is irradiated

(26) Evans, J. F.; Kuwana, T. *Anal. Chem.* **1977**, *49*, 1632.
(27) Tse, D. C. S.; Kuwana, T. *Anal. Chem.* **1978**, *50*, 1315.
(28) Moiroux, J.; Elving, P. J. *Anal. Chem.* **1978**, *50*, 1056.
(29) Kamau, G. N.; Willis, W. S.; Rusling, J. F. *Anal. Chem.* **1985**, *57*, 545.
(30) Thornton, D. C.; Corby, K. T.; Spendel, V. A.; Jordan, J.; Robbat, A.; Rutstrom, D. J.; Gross, M.; Ritzler, G. *Anal. Chem.* **1985**, *57*, 150.
(31) Morcos, I.; Yeager, E. *Electrochim. Acta* **1970**, *15*, 953.
(32) Packard, R. T.; McCreery, R. L. *Anal. Chem.* **1987**, *59*, 2631.
(33) Nemanich, R. J.; Lucovsky, G.; Solin, S. A. *Materials Sci. Eng.* **1977**, *31*, 157.
(34) Nemanich, R. J.; Solin, S. A. *Phys. Rev. B* **1979**, *20*, 392.
(35) Vidano, R. P.; Fischbach, D. B.; Willis, L. J.; Loehr, T. M. *Solid State Commun.* **1981**, *39*, 341.
(36) Nakamizo, M.; Tamai, K. *Carbon* **1984**, *22*, 197.
(37) Vidano, R.; Fischbach, D. B. *J. Am. Cer. Soc.* **1978**, *61*, 13.
(38) Tuinstra, F.; Koenig, J. L. *J. Chem. Phys.* **1970**, *53*, 1126.
(39) McQuillan, A. J.; Hester, R. E. *J. Raman Spectrosc.* **1984**, *15*, 15.
(40) Nakamizo, M.; Kammereck, R.; Walker, P. L. *Carbon* **1974**, *12*, 259.
(41) Braunstein, G.; Dreselhaus, M. S., et al. *Materials Res. Symp. Proc.* **1986**, 233.
(42) Tsu, R.; Gonzales, J.; Hernandez, I. *Solid State Commun.* **1978**, *27*, 507.
(43) Dresselhaus, M. S.; Dresselhaus, G. *Adv. Phys.* **1981**, *30*, 139.
(44) Nakamizo, M.; Honda, H.; Inagaki, M. *Carbon* **1978**, *16*, 281.
(45) Dresselhaus, M. S.; Dresselhaus, G. *Adv. Phys.* **1981**, *30*, 290–298.

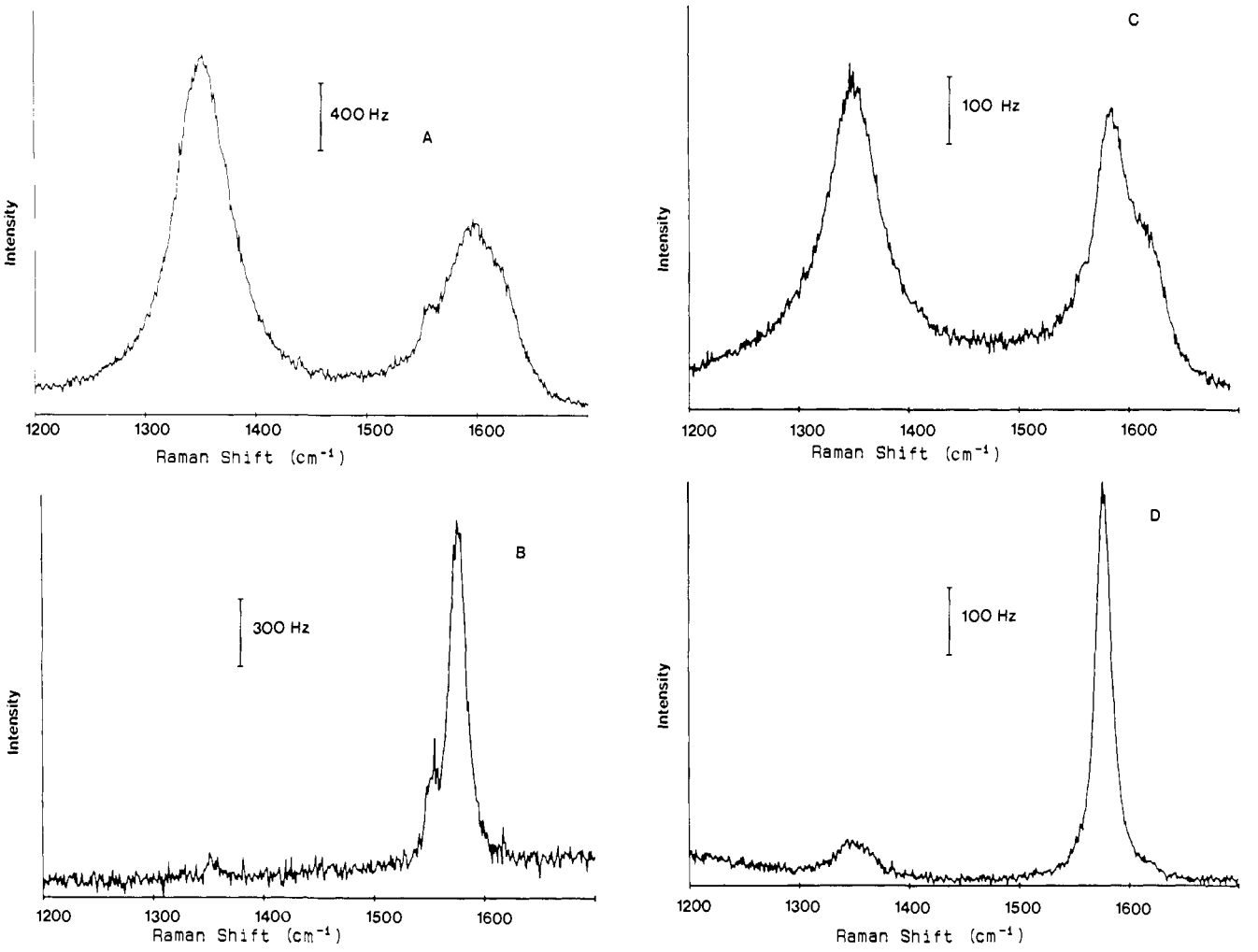


**Figure 1.** Raman spectra of various forms of carbon, obtained with 515-nm laser light. A and B are gross spectra of GC-20S and HOPG basal plane, respectively, 20 mW at sample covering a 0.1 × 1 mm spot. Spectral resolution was 10 $cm^{-1}$. Shoulder at 1565 $cm^{-1}$ is dioxygen in the room air in which spectra were obtained. C and D are microprobe spectra of the HOPG edge plane and a visible defect on the HOPG basal plane, respectively, obtained with 5 mW of laser light on a ca. 5 $\mu$m diameter spot.

with Nd:YAG pulses of varying power, dramatic changes occur in the voltammetry and Raman spectra. At laser peak powers equal to and above 45 MW $cm^{-2}$, the 1360-$cm^{-1}$ band appears in the Raman spectra of the irradiated region, as shown in Figure 4. The spectrum of the irradiated area was obtained with the microprobe on a region similar to the gray area apparent in the SEM of Figure 2B. The spectrum was essentially uniform across the laser-treated area, and no significant differences were observed between gross and microprobe spectra. No distinct 1620-$cm^{-1}$ band was observed for laser-treated surfaces, but a weak shoulder on the 1582-$cm^{-1}$ band was observed at 45 MW $cm^{-2}$ and above. The voltammetric peak separation for $Fe(CN)_6^{3-/4-}$ and dopamine decreased strongly at 45 MW $cm^{-2}$ and above, as shown in Figure 3. The effect occurred suddenly between 40 and 50 MW $cm^{-2}$, with no intermediate peak separations between the two extremes. Figure 5 summarizes the gross Raman intensity data and voltammetric $\Delta E_p$ values for dopamine and $Fe(CN)_6^{3-/4-}$. Assuming a value of $\alpha = 0.5$ for $Fe(CN)_6^{3-/4-}$, the increase in rate constant upon laser activation at 45 MW $cm^{-2}$ was from $<10^{-9}$ to $1.7 \times 10^{-3}$ cm $s^{-1}$, as determined from $\Delta E_p$.[46]

The SEM obtained from surfaces after laser treatment in air shows no structure or spatial heterogeneity, only a "grey" region corresponding to the laser spot (Figure 2B).

**Electrochemical Pretreatment of HOPG.** The SEM of electrochemically pretreated HOPG in Figure 2C exhibits a complex pattern of defects, which may emanate from a few points on the surface. These complex defect networks were surrounded by sometimes large (~20 $\mu$m) regions of apparently undamaged HOPG. The bright lines associated with defects may be edge planes, but their brightness implies electron beam charging and perhaps some insulating character. Figure 6 shows the effect of ECP at three potentials on the gross Raman spectra of fresh HOPG surfaces. Spectrum B exhibits a 1605-$cm^{-1}$ band which first appears at a pretreatment potential of about 1.6 V. In addition, the 1360-$cm^{-1}$ band appears and becomes more intense as the ECP potential is increased. These modes indicate that the initial nearly defect free HOPG surface is delaminating and fracturing, resulting in smaller crystallites. The 1605- and 1360-$cm^{-1}$ bands do *not* vary together, however, showing different onset potentials, and occasionally varying in opposite directions. Three microprobe spectra of an HOPG surface pretreated at 1.85 V are shown in Figure 7. Some regions sampled by the 5 $\mu$m laser spot exhibit both the 1360- and 1620-$cm^{-1}$ bands, but translation of the microprobe to a region only 20 $\mu$m away yields a spectrum without the 1360-$cm^{-1}$ band. The Raman microprobe indicates spatial heterogeneity on a scale of tens of microns for a surface treated at 1.85 V. The effect of ECP on the electrochemical properties of the HOPG surface is apparent by comparing curves A and B in Figure 8. The 1.85-V ECP has activated dopamine and $Fe(CN)_6^{3-/4-}$ dramatically, with both systems showing large reductions in $\Delta E_p$. The existence of two voltammetric waves for dopamine and the distortion of the $Fe(CN)_6^{3-/4-}$ wave imply spatial heterogeneity on a scale larger than $(Dt)^{1/2}$ ($D$ = diffusion coefficient, $t$ = approximate scan time through voltammetric wave). For the scan rate employed, $(Dt)^{1/2}$ is about 25 $\mu$m, implying that activated regions are separated from each other by at least this distance.

(46) Nicholson, R. S. *Anal. Chem.* **1965**, *37*, 1351.

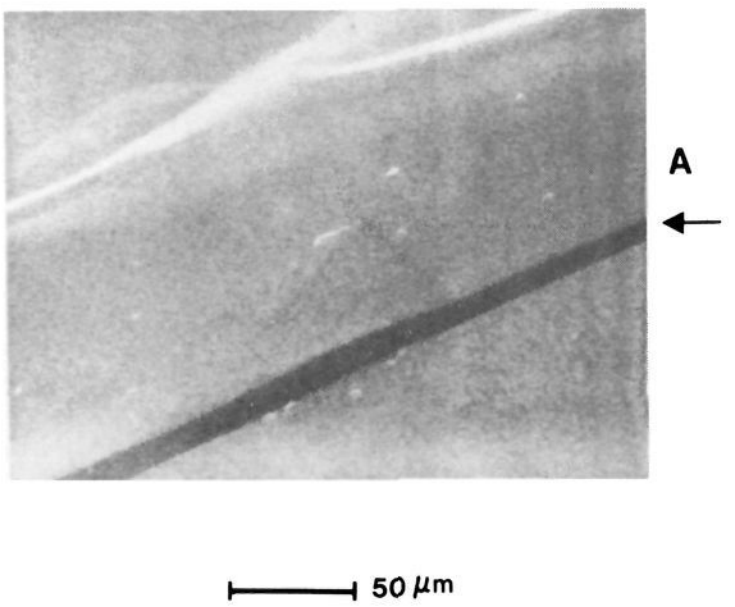


**Figure 2.** SEM's of carbon samples obtained in secondary electron mode. (A) Freshly cleaned HOPG with arrow indicating a defect similar to that exhibiting spectrum D of Figure 1. (B) Laser treated (50 MW $cm^{-2}$, 1064 nm, 3 pulses) HOPG. The gray area is the laser spot, and the large defect to the right was present before laser treatment and served as a marker. Laser treatment occurred in air. (C) Electrochemically pretreated HOPG (1.95 V vs AgCl, 2 min, 0.1 M $KNO_3$).

Both the gross Raman spectrum and microprobe spectra of HOPG after a 1.95-V ECP have the appearance of Figure 6C. Unlike the 1.85-V ECP, the 1.95-V surface exhibits no spatial heterogeneity and shows only slight variation in the Raman spectrum for many microprobe positions on the activated surface. The voltammetry of dopamine and $Fe(CN)_6^{3-/4-}$ on the more vigorously activated surface (Figure 8) shows full activation, with no observed peak from an inactive region. Thus, any spatial heterogeneities are small relative to the microprobe spot size (5 μm) or $(Dt)^{1/2}$ for a 0.2 V/s voltammogram.

With use of the conventional laser spot size (100 μm × 1 mm), spatially averaged Raman spectra were obtained for several ECP potentials. Figure 9 shows the 1360- and 1605-$cm^{-1}$ intensities

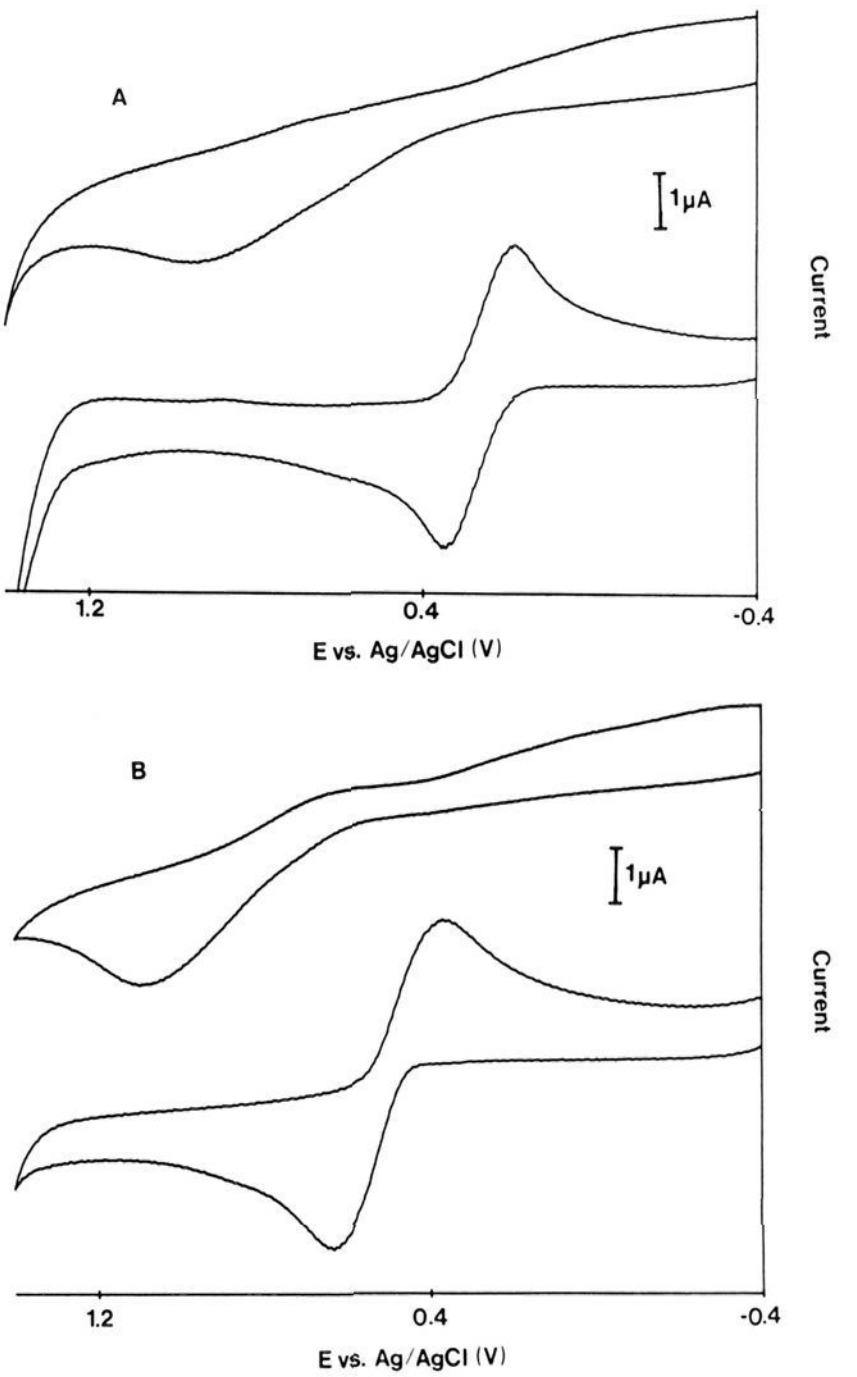


**Figure 3.** Voltammograms of dopamine and $Fe(CN)_6^{3-/4-}$ on untreated and laser-treated HOPG: (A) $Fe(CN)_6^{3-/4-}$, 1 M KCl, 0.2 $V/s^{-1}$; (B) dopamine in 0.1 M $H_2SO_4$, 0.2 V $s^{-1}$. Upper curve in both cases is before laser treatment, and lower curves are after laser treatment (50 MW $cm^{-2}$, 3 pulses). Laser treatment was performed in air before immersion in electrochemical solutions.

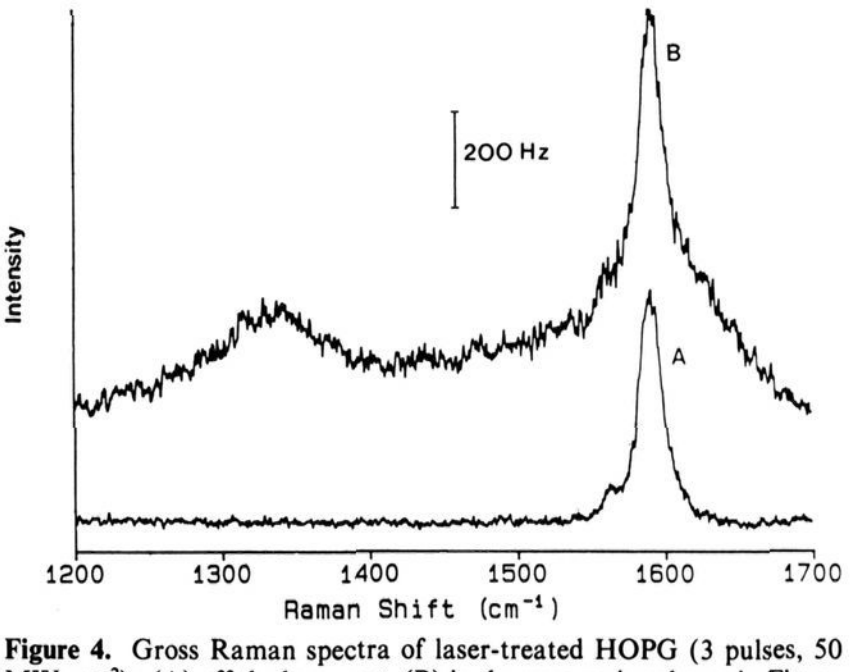


**Figure 4.** Gross Raman spectra of laser-treated HOPG (3 pulses, 50 MW $cm^{-2}$): (A) off the laser spot, (B) in the gray region shown in Figure 2B.

relative to the 1582-$cm^{-1}$ band for a large observation area as a function of pretreatment potential. The $I_{1360}/I_{1585}$ ratio indicates the spatially averaged intensity of the $A_{1g}$ mode within the sampled area. Figure 9 also shows the $\Delta E_p$ for $Fe(CN)_6^{3-/4-}$ as a function of ECP potential. The dramatic decrease in $\Delta E_p$ coincides with

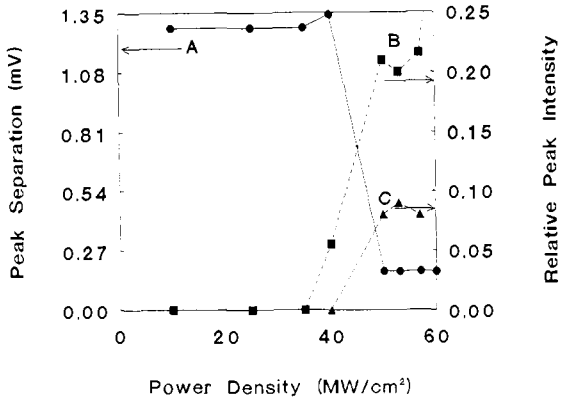


**Figure 5.** Effect of laser power density on $\Delta E_p$ for $Fe(CN)_6^{3-/4-}$ (curve A), intensity ratio of 1360 to 1582 $cm^{-1}$ gross Raman band (curve B), and intensity ratio of 1605 to 1582 $cm^{-1}$ band (curve C). Three laser pulses in air, and spectra obtained in air. Data in curve C are approximate due to the difficulty of determining the intensity of the 1605-$cm^{-1}$ shoulder.

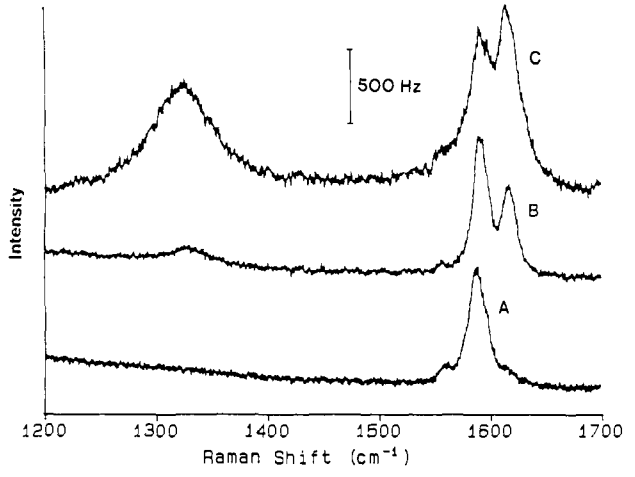


**Figure 6.** Gross Raman spectra obtained in air after electrochemically pretreating HOPG for 2 min in 0.1 M $KNO_3$, 1565-$cm^{-1}$ peak is dioxygen: (A) 1.6 V vs Ag/AgCl; (B) 1.85 V; (C) 1.95 V. Laser spot on surface was 0.1 × 1 mm in size.

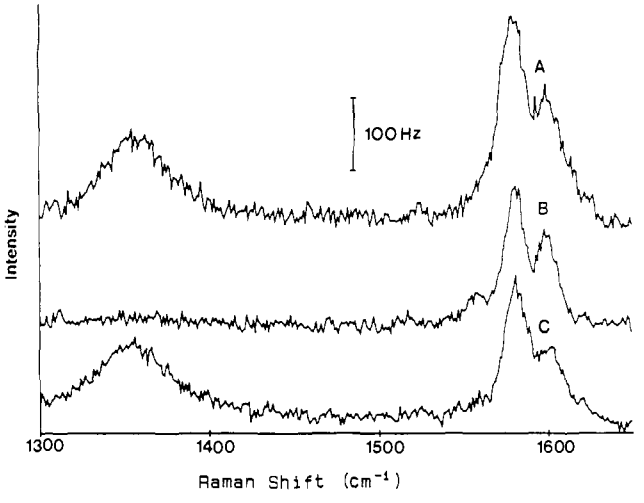


**Figure 7.** Raman microprobe spectra of HOPG electrochemically pretreated at 1.85 V. Same conditions as Figure 6 except the laser spot size on surface was ca. 5 $\mu$m in diameter. Spectra B and C were obtained on the same surface as A, after two successive ~20-$\mu$m translations of the microprobe.

the increase in the 1360-$cm^{-1}$-band intensity. In addition, the 1605-$cm^{-1}$ intensity occurs after ECP potentials significantly lower than those required for electron transfer activation. The $k^0$ for $Fe(CN)_6^{3-/4-}$ observed for ECP potentials below 1.6 V was $<10^{-9}$ cm/s, while that for the 1.95-V ECP was $6.5 \times 10^{-3}$ cm $s^{-1}$.

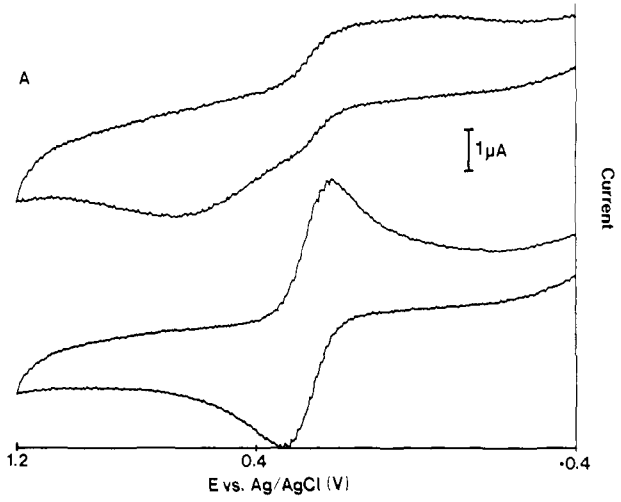


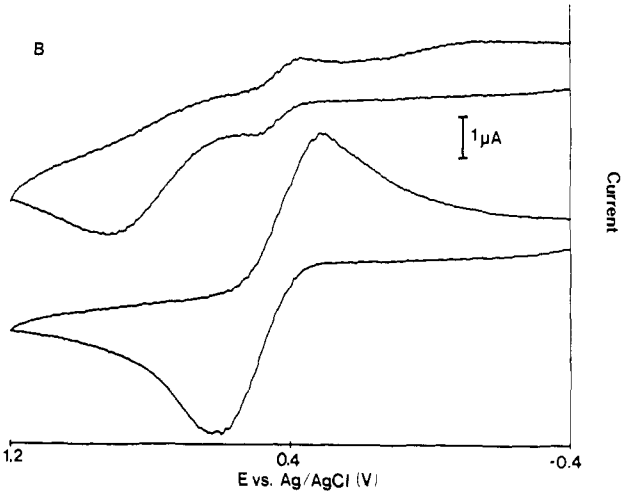


**Figure 8.** Cyclic voltammetry after ECP of HOPG, with the same voltammetric conditions as Figure 3. ECP was for 2 min in 0.1 M $KNO_3$. (A) $Fe(CN)_6^{3-/4-}$, (B) dopamine. Upper curve in both cases is after 1.85-V ECP, lower curves after 1.95-V ECP.

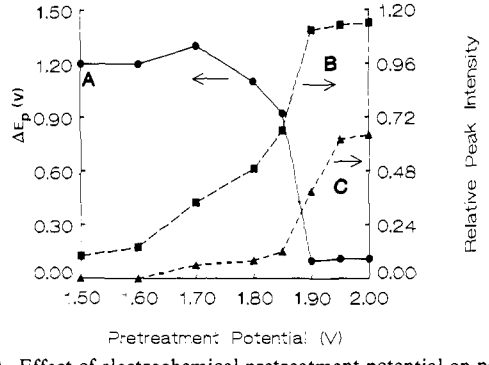


**Figure 9.** Effect of electrochemical pretreatment potential on peak separation for $Fe(CN)_6^{3-/4-}$ in 1 M KCl (curve A), 1605 $cm^{-1}$/1582 $cm^{-1}$ Raman intensity ratio, (curve B), and 1360 $cm^{-1}$/1582 $cm^{-1}$ peak intensity ratio (curve C). $\Delta E_p$ was determined on HOPG for $Fe(CN)_6^{3-/4-}$ in 1 M KCl after ECP in 0.1 M $KNO_3$ for 2 min. Pretreatment potentials are relative to Ag/AgCl.

## Discussion

The Raman spectra of laser treated HOPG indicate a damage mechanism with a well-defined threshold. The sudden appearance of the 1360-$cm^{-1}$ band at power densities above 45 MW $cm^{-2}$ demonstrates laser induced fragmentation of the graphitic lattice, resulting in edge plane defects in the initially smooth HOPG basal plane. Compared to ECP, the laser treated surface exhibits weak 1605-$cm^{-1}$ intensity, implying that little or no delamination of

Table I. Electron Transfer Kinetics for $Fe(CN)_6^{3-/4-}$ on Activated Carbon Surfaces

| electrode | electrolyte | $\Delta E_p$ | scan rate, V/s | $k^0$, cm/s | $I_{1360}/I_{1585}$ | ref |
|---|---|---|---|---|---|---|
| HOPG, basal[a] | 0.5 M $K_2SO_4$ | 710 mV | 0.1 | $<10^{-7}$ [b] | ~0[c] | 7 |
| HOPG, edge | 0.5 M $K_2SO_4$ | 190 mv | 0.1 | 0.0015[b] | 1.1[c] | 7 |
| HOPG, basal | 1.0 M KCl | >1.2 V | 0.1 | $<10^{-9}$ | ~0 | this work |
| HOPG,[a] laser, 50 MW $cm^{-2}$ | 1.0 M KCl | 175 mV | 0.1 | 0.0018 | 0.20 | this work |
| HOPG, ECP 1.4 V, 15 min citrate buffer | 0.5 M $K_2SO_4$ | 190 | 0.1 | 0.0015[b] | | 7 |
| HOPG, ECP 1.9 V, 2 min 0.1 M $KNO_3$ | 1 M KCl | 105 | 0.1 | 0.0063 | 0.60 | this work |
| GC-20, heat treated | 1 M KCl | 65 | 1.0 | 0.14[b] | | 6 |
| GC-20, polished | 1 M KCl | | | 0.14 | | 10 |
| GC-20, laser treated | 1 M KCl | | | 0.20 | 2.1[c] | 21 |

[a] All entries for HOPG refer to basal plane unless noted otherwise. [b] Calculated from published data, assuming $D = 6.3 \times 10^{-6}$ $cm^2$ $s^{-1}$. [c] Results from this work.

graphite planes occurs. In addition, the spatial homogeneity of the 1360-$cm^{-1}$ band is consistent with SEM results, indicating a homogeneously damaged basal plane, at least down to the microprobe spot size (<5 μm). Based on the correlation between Raman intensity ratio and crystallite size,[38] the 0.2 ratio of the 1360- to 1582-$cm^{-1}$ peak observed for laser-treated HOPG implies a mean crystallite size well below $(Dt)^{1/2}$ for any conventional voltammetric experiment.

The sudden increase in 1360-$cm^{-1}$-band intensity correlates with a large improvement in electron transfer kinetics, with $k^0$ for $Fe(CN)_6^{3-/4-}$ increasing by at least six orders of magnitude between 40 and 50 MW $cm^{-2}$. Several $k^0$ values are listed in Table I, along with relevant values from the literature. Despite unavoidable uncertainties due to variations in surface cleanliness and preparation, certain deductions are possible from Table I. The laser activated HOPG basal plane exhibits a $k^0$ which is comparable to that of edge plane but lower than properly prepared GC or electrochemically pretreated HOPG. The association between edge plane density and increased $k^0$ for the laser-treated surface is obvious from Figure 5, with the presence of the 1360-$cm^{-1}$ band being a prerequisite for electron transfer activation.

The electrochemically treated HOPG surface exhibits the 1360-$cm^{-1}$ band after treatment at sufficiently high potentials, but ECP also produces a 1605-$cm^{-1}$ band. This band is associated with delamination of the graphitic planes, either by intercalation[43] or by "severe disorder".[35,36] The shift from 1582 to 1600–1630 $cm^{-1}$ upon intercalation is largely independent of the charge of the intercalant,[43] implying that it is not due to an electronic effect on the grapitic π system. Since the intensities of the 1605- and 1582-$cm^{-1}$ peaks are roughly equal, the graphite probed by the laser beam has approximately equal populations of graphite planes with two adjacent planes and those with only one. Given the penetration depth of the sampling laser beam (ca. 50–100 graphite layers), it is possible that the 1582-$cm^{-1}$ band results from underlying unmodified HOPG while the modified surface layers show only the 1605-$cm^{-1}$ band. While intercalation is a possible source of the 1605-$cm^{-1}$ band, such intercalation compounds should not be stable in the neutral or weakly acidic pretreatment solution.[4] In most cases, the redox potential for intercalation is higher than that for carbon or water oxidation, so that intercalation compounds should not exist in the ECP solution. However, the oxidation of GC30 glassy carbon at elevated temperature in air can lead to a 1620-$cm^{-1}$ band,[36] perhaps because the oxidation of graphite edges forces delamination. On the basis of the literature and current results, oxidation induced delamination appears most likely as the origin of the 1605-$cm^{-1}$ band for electrochemically pretreated HOPG.

The 1360-$cm^{-1}$ band observed upon ECP has a higher onset potential than the 1605-$cm^{-1}$ band (for ECP in 0.1 M $KNO_3$) and is indicative of fracturing of the graphite planes rather than delamination. As was the case with laser treatment, the 1360-$cm^{-1}$ band is closely coupled with enhanced electron transfer. As is apparent from Figure 9, the 1360/1582 intensity ratio must be above about 0.1 to achieve enhanced $k^0$ for $Fe(CN)_6^{3-/4-}$. The presence of the 1605-$cm^{-1}$ band does not ensure a fast $k^0$; in fact, an electrode showing a fairly large 1620-$cm^{-1}$ peak (at 1.8-V ECP, for example) still has very slow electron transfer. For a laser treated surface (Figure 4B), the 1605-$cm^{-1}$ band is small ($I_{1605}/I_{1360} < 0.1$), but a high $k^0$ is observed. Thus, the 1605-$cm^{-1}$ band does not correlate with high $k^0$ for either laser or electrochemical pretreatment. In contrast, the 1360-$cm^{-1}$ band always correlates with high $k^0$, for both laser and ECP. One concludes that graphitic edge plane is necessary for fast $k^0$, and delamination (whether or not intercalation occurs) is not required for fast $k^0$.

For those surfaces where data are available, the presence of the 1360-$cm^{-1}$ band is correlated with improved electron transfer kinetics. As shown in Table I, laser treatment of HOPG over the laser power range employed leads to a maximum 1360/1582 intensity ratio of 0.2, and a $k^0$ of $1.8 \times 10^{-3}$ cm $s^{-1}$ ($\Delta E_p$ = 175 mV). These values are consistent with the ECP results, where a 1360/1582 ratio of 0.2 would imply a $\Delta E_p$ of 0.2–0.3 V. When ECP produces a higher 1360/1582 ratio (0.4–0.6), a lower $\Delta E_p$ (105 mV) and higher $k^0$ ($6.5 \times 10^{-3}$ cm $s^{-1}$) are observed. Even though laser and ECP are very differnt means to alter the surface, with presumably very different mechanisms, they both show similar $k^0$ values when similar 1360-$cm^{-1}$-band intensities are observed. In addition, laser-activated GC-20 exhibits the highest 1360/1582 ratio (2.1) and the highest $k^0$ (0.20 cm $s^{-1}$). The results presented in Table I are not sufficient to deduce a quantitative relationship between Raman intensity ratios and observed $k^0$, but it is clear that high $k^0$ and high 1360-$cm^{-1}$-band intensity are correlated for several materials in addition to basal plane HOPG. In order for such a relationsihp to be observed, we would predict that surfaces of equal cleanliness are required, so that carbon microstructure is the only variable involved.

The spatial heterogeneity of the HOPG surface following a 1.85-V ECP is apparent from both Raman microprobe and voltammetric data. Untreated HOPG shows widely separated regions with observable 1360-$cm^{-1}$ bands, but these are only present on visible defects which comprise less than 1% of the total surface area. After a 1.85-V ECP, regions with 1360-$cm^{-1}$ intensity are more frequent, but they are separated on the surface by tens of microns. At higher ECP potential, the 1360-$cm^{-1}$ band is uniformly present on the surface, and the voltammetry exhibits a single, activated redox couple. It may be significant that not all defects visible by light microscopy showed the 1360-$cm^{-1}$ Raman band. However, the spatial heterogeneity observed for both the 1360-$cm^{-1}$ band and fast $k^0$ supports the association between an electrochemically active surface and graphitic edge plane defects.

While ECP undoubtedly creates oxygen-containing functional groups on the carbon surface, the role of oxygen in the spectral and electrochemical results of ECP is unclear. None of the three Raman bands shift when the ECP is carried out in $H_2{}^{18}O$, indicating that surface oxygen is weakly coupled to the observed vibrational modes. Furthermore, carbon materials that contain little or no known oxygen (e.g., GC30, ground graphite) exhibit any or all of the 1360-, 1620-, and 1582-$cm^{-1}$ bands.[36,37] As reported for vacuum heat treatment and laser activation, surfaces with immeasurably low surface oxygen content (as determined from ESCA) can exhibit fast $k^0$ for ascorbic acid, $Fe(CN)_6^{3-/4-}$, and dopamine.[6,8,22,24] The absence of a role of oxygen in the activation process is substantiated by the laser pretreatment. The laser has been shown to reduce surface oxygen on GC, even in water,[22] and the laser pulse is not a fundamentally oxidative process

like ECP. The laser does activate the surface, however, and the activation correlates with the 1360-$cm^{-1}$-band intensity. Thus, the correlation between activation and Raman spectral properties is consistent, while neither the spectrum nor activation correlate with oxygen content. There is no doubt that formation of an oxide film by ECP results in activation,[12,14,16,17,20] and it has been shown that the oxide film thickness correlates with the extent of activation.[20] However, activation by ECP appears to result from oxidation-induced fracturing of the graphite lattice rather than any more direct effect of surface oxides on heterogeneous electron transfer.

While both laser and ECP result in similar changes in the Raman spectrum and similar $k^0$ activation, it is the differences between them that provide insight into the activation mechanism. Since HOPG is initially very clean and is quite inert toward adsorption, activation of HOPG probably does not involve surface cleaning. Both laser and ECP create defects in the HOPG surface that result in the edge plane Raman peak and increased $k^0$, but the two pretreatments differ in the spatial distribution of defects. ECP leads initially to widely spaced defects while the laser appears to create an even distribution of both the 1360-$cm^{-1}$ Raman peak and electrochemically active sites. The observations are consistent with a nucleation mechanism for defect growth during ECP. The few defects on fresh HOPG may act as nuclei for the delamination and fracturing of nearby graphite planes. As implied earlier, it is quite possible that the formation of surface oxides during ECP produces strain on the graphite lattice which produces fracturing and delamination. The result is spatially separated active regions, at least at a low ECP potential. At higher potentials, defect growth extends over the entire surface, and uniform activation and 1360-$cm^{-1}$-band intensity result. The absence of spatial heterogeneity on a greater than micron scale for laser-treated HOPG implies that the laser-induced temperature excursion or associated mechanical strains create many defects that do not grow from a few nuclei. Given the 10-ns duration of the laser pulse compared to the 2-min ECP, a slow nucleation and growth process may not be possible for laser treatment. The fact that rate enhancement and 1360-$cm^{-1}$-band intensity occur suddenly and completely at between 40 and 50 MW $cm^{-2}$ may imply that laser-induced thermal stresses shatter the graphite lattice, leading to a fine network of edge plane defects but little delamination or surface oxidation.

To our knowledge, these results constitute the first correlation of a surface feature observable with vibrational spectroscopy and electron transfer activation on carbon electrodes. The rate enhancement is monotonic with the 1360 $cm^{-1}$ Raman band associated with edge plane graphite with higher edge plane density always correlating with higher $k^0$. The important question of the mechanism by which edge plane defects enhance electron transfer remains open. The basal plane of HOPG exhibits some properties of a semiconductor electrode, particularly anomalously low capacitance due to space charge effects.[47] On the basis of the *c*-axis resistivity of 0.15 Ω·cm, the internal resistance of the working electrode for our geometry is <1 Ω and is not sufficient to significantly increase the observed $\Delta E_p$. However, the low density of states at the fermi level for an HOPG basal plane in solution may lead to a lower $k^0$ value.[47] It is possible that the disruption of the basal plane by ECP or laser treatment destroys its semiconductor character and permits faster electron transfer. An alternative explanation is the requirement of edge plane sites for electron transfer, independent of any semiconductor properties. In either case, Raman spectroscopy has provided a correlation between edge defects and $k^0$ enhancement. In addition, we have established that ECP and laser activation are effective only under conditions where edge plane is created.

These conclusions do not rule out other activation mechanisms for certain chemical systems. Only $Fe(CN)_6^{3-/4-}$ and dopamine activation have been correlated with edge plane density in the current work, and there may be other redox systems where redox mediation by functional groups (e.g., quinones)[26,27] or proton transfer may be involved.[16] While these mechanisms may indeed be important for several electrocatalytic reactions, there is no evidence that proton transfer or oxygen functional groups are important for activation of HOPG toward $Fe(CN)_6^{3-/4-}$ and dopamine by laser or ECP. The most convincing evidence against their involvement is the independence of vacuum heat treatment[6,8] or laser activation[23,24] on surface oxygen content.

While HOPG was chosen for this work as a well-defined example of carbon electrodes, it is useful to consider the applicability of the result to more commonly used materials such as glassy carbon. The lower power density required for laser activation of GC[22] probably results from its lower reflectivity compared to HOPG, with attendant higher energy absorption. Polished GC will have many exposed edge plane defects, and the width of basal plane crystallites will be very small, typically less than 100 Å.[48] Despite the major differences in microstructure, the delamination and fracturing observed for HOPG upon ECP would still be expected for similar treatment of GC. The processes would presumably occur in parallel with surface oxidation. Assuming the same conclusions reached for HOPG are valid for GC, the surface oxidation is not required for activation, but fracturing and site formation are. However, the surface oxidation and perhaps removal of GC layers may also serve to clean the GC surface of impurities which impede electron transfer. HOPG surfaces are inherently clean but are largely inactive until edge planes are created. GC already has edge plane defects, but it must be cleaned to expose these edge planes. The relative importance of surface cleaning and microstructural changes to the activation of GC is not yet established, and experiments directed toward this end are currently under way. The relationship between carbon microstructure and electron transfer activity reported here will only be observed when variables related to surface cleanliness are removed.

**Acknowledgment.** The efforts on carbon activation and electrochemical characterization (R.J.B.) were supported by the Air Force Office of Scientific Research. Development and application of Raman spetroscopy techniques (R.T.P.) was funded by the Chemical Analysis Division of the National Science Foundation. The authors thank A. W. Moore of Union Carbide (Parma, Ohio) for the HOPG samples used througout the project.

**Note Added in Proof.** A recent report (Gewirth, A. A.; Bard, A. J. *J. Phys. Chem.* **1988**, *92*, 5563) has also concluded a nucleation and growth mechanism for ECP of HOPG, based on scanning tunnelling microscopy.

**Registry No.** HOPG, 7782-42-5; GC, 7440-44-0; $KNO_3$, 7757-79-1; $Fe(CN)_6^{4-}$, 13408-63-4; $Fe(CN)_6^{3-}$, 13408-62-3; dopamine, 51-61-6.

(47) Randin, J.-P. In *Encyclopedia of Electrochemistry of the Elements*; Bard, A. J., Ed.; Delcher: New York, 1976; Vol. 7, pp 12–21, 238–239.

(48) Jenkins, G. M.; Kawamura, K. *Nature* **1971**, *231*, 175.